Published in final edited form as:
*Mol Cell*. 2014 May 22; 54(4): 613–625. doi:10.1016/j.molcel.2014.03.043.

# A Role for WDR5 in Integrating Threonine 11 Phosphorylation to Lysine 4 Methylation on Histone H3 during Androgen Signaling and in Prostate Cancer

**Ji-Young Kim**[1], **Taraswi Banerjee**[1], **Aurimas Vinckevicius**[1], **Qianyi Luo**[3], **J. Brandon Parker**[1], **Mairead R Baker**[4], **Ishwar Radhakrishnan**[3], **Jian-Jun Wei**[2,5], **Grant D. Barish**[4,5], and **Debabrata Chakravarti**[1,5,*]

[1]Division of Reproductive Science in Medicine, Department of OB/GYN, Northwestern University, Evanston, IL, 60208

[2]Department of Pathology, Northwestern University, Evanston, IL, 60208

[3]Department of Molecular Biosciences, Northwestern University, Evanston, IL, 60208

[4]Division of Endocrinology, Metabolism and Molecular Medicine, Department of Medicine, Northwestern University, Chicago, Illinois 60611

[5]Robert H. Lurie Comprehensive Cancer Center, Feinberg School of Medicine, Northwestern University, Chicago, Illinois 60611

## SUMMARY

Upon androgen stimulation, PKN1-mediated histone H3 threonine 11 phosphorylation (H3T11P) promotes AR target genes activation. However, the underlying mechanism is not completely understood. Here, we show that WDR5, a subunit of the SET1/MLL complex, interacts with H3T11P and this interaction facilitates the recruitment of the MLL1 complex and subsequent H3K4 trimethylation (H3K4me3). Using ChIP-seq, we find that androgen stimulation results in a



* To whom correspondence should be addressed: Debabrata Chakravarti Northwestern University Feinberg School of Medicine 303 E Superior St. Lurie 4-119 Chicago, IL 60611 debu@northwestern.edu Fax: 312-503-0095.



The authors declare no conflicts of interests.

Authors' contributions are as follows: DC conceived the research plan. J-YK, TB, JBP, and DC designed experiments. J-YK, TB, AV, QL, JBP and MRB generated reagents and/or performed research. J-YK, IR, J-JW, JBP, GB, and DC analyzed data. GB and DC analyzed genome-wide data. J-JW analyzed IHC data. IR analyzed ITC data. DC and J-YK wrote the manuscript with help from AV, JBP, IR, and GB. All authors reviewed and edited the manuscript.

SUPPLEMENTAL INFORMATION

Supplemental Information includes seven figures, and two tables, Supplemental Experimental Procedures, Supplemental Reference, and can be found with this article online at http:. Supplemental Experimental Procedures contain information on antibodies, plasmids and cloning, retrovirus production and transduction, production of recombinant protein, *in vitro* transcription and translation, GST-pull down assay, isothermal titration calorimetry, immunoprecipitation and immunoblot analysis, and reverse transcription and qPCR, and detailed information on cell culture and treatment, histone peptide pull down assays and protein identification by MS, nuclear and nucleosomal protein preparation, ChIP assays and sequential ChIP, BrdU and AlamarBlue cell proliferation assay, and immunohistochemistry and TMAs.

six-fold increase in the number of H3T11P-marked regions and induces WDR5 colocalization to one third of H3T11P-enriched promoters, thus establishing a genome-wide relationship between H3T11P and recruitment of WDR5. Accordingly, PKN1 knock-down or chemical inhibition severely blocks WDR5 association and H3K4me3 on AR target genes. Finally, WDR5 is critical in prostate cancer cell proliferation, and is hyperexpressed in human prostate cancers. Together, these results identify WDR5 as a critical epigenomic integrator of histone phosphorylation and methylation and a major driver of androgen-dependent prostate cancer cell proliferation.

## INTRODUCTION

Androgen receptor (AR) plays important roles as a transcription factor in prostate cancer development and progression (Izumi et al., 2013; Schrecengost and Knudsen, 2013; Shafi et al., 2013; Takayama and Inoue, 2013). Upon binding to androgens in the cytoplasm, AR dimerizes, relocates to the nucleus, and binds DNA at androgen response elements (AREs) where it regulates transcription by recruiting coactivators or corepressors and chromatin remodeling and modifying complexes (Dasgupta et al., 2014; Perissi et al., 2010; Rosenfeld and Glass, 2001; Shang et al., 2002). Chromatin modifications, such as histone acetylation, methylation, phosphorylation, ubiquitylation, and ADP ribosylation, have been found to play crucial roles in gene expression and other chromatin based processes (Banerjee and Chakravarti, 2011; Bannister and Kouzarides, 2011; Campos and Reinberg, 2009; Chi et al., 2010; Loomis et al., 2009; Musselman et al., 2012; Nowak and Corces, 2004; Preuss et al., 2003; Shimada et al., 2008; Suganuma and Workman, 2011).

Recently, the Schüle laboratory demonstrated that phosphorylation of histone H3 at threonine 11 (H3T11P) is important for androgen-dependent transcription in prostate cancer cells (Metzger et al., 2008). Upon androgen stimulation, AR and protein kinase C-related kinase 1 (PKN1, previously known as PRK1) associate with AR target genes resulting in H3T11 phosphorylation. Furthermore, PKN1 kinase activity promotes demethylation of H3 trimethylated at lysine 9 (H3K9me3) – a chromatin mark associated with transcriptional repression and heterochromatin formation – via cooperative action of lysine-specific histone demethylases KDM4C/JMJD2C and KDM1A/LSD1 (Metzger et al., 2008; Wissmann et al., 2007). However, genome-wide distribution of H3T11P as well as the role of PKN1-mediated H3T11 phosphorylation in regulating further deposition of activating histone marks, like histone H3 lysine 4 (H3K4) methylation remain unclear.

Mono-, di-, and trimethylation of H3K4 mark the promoter and enhancer regions of actively transcribed genes (Calo and Wysocka, 2013; Eissenberg and Shilatifard, 2010). These histone modifications are deposited by the SET1/MLL histone methyltransferase (HMTase) complex, which, at its core, is composed of either KMT2A/MLL1, KMT2B/MLL2, KMT2C/MLL3, KMT2D/MLL4, SETD1A, or SETD1B associated with WRAD module (WDR5, RBBP5, ASH2L, and DPY30), and other variable partners (Patel et al., 2008; Shilatifard, 2012; van Nuland et al., 2013). Interestingly, WDR5 binds both unmodified and methylated H3K4 *in vitro* and is required for the trimethylation of this residue by SET1/MLL complex (Dou et al., 2006; Steward et al., 2006; Wysocka et al., 2005). Less

clear is the understanding of signal dependent recruitment of SET1/MLL complex on target genes.

In this study, we discovered that WDR5 (WD repeat-containing protein 5) directly interacts with H3T11P *in vitro* and colocalizes with H3T11P *in vivo* on AR regulated genes upon androgen stimulation. Under these conditions, we also observed significant overlap between WDR5 and H3T11P localization on a genome-wide scale. Mechanistically, we determined that, in response to androgen treatment, PKN1 and H3T11P facilitate recruitment of WDR5 and the associated MLL1 complex that lead to subsequent trimethylation of H3K4 at AR target genes. Consequently, depletion of WDR5 blocked transcriptional activation of AR target genes as well as androgen-dependent proliferation of LNCaP cells. Finally, we found that WDR5 is highly expressed in prostate cancers when compared to normal prostate epithelium. Collectively, these data describe a novel role of WDR5 and its interaction with H3T11P in androgen signaling, leading to further chromatin modifications, and they implicate WDR5 in prostate cancer cell proliferation.

## RESULTS

### Histone H3 threonine 11 phosphorylation facilitates WDR5 interaction*in vitro*

Using unmodified or threonine 11 phosphorylated peptides encompassing histone H3 amino acids 1-21 as affinity matrices, we performed peptide pull-down assays on HeLa S3 nuclear extracts to identify H3T11P associated proteins (Figures S1A and S1B). Differentially bound proteins were analyzed by matrix-assisted laser desorption-ionization time-of-flight mass spectrometry (MALDI-TOF MS/MS). One of the proteins retained on H3T11P peptides was identified as WDR5, a subunit of the SET1/MLL complex (Figure 1A and Figure S1C). Because we wanted to study the effects of H3T11P in prostate cancer cells, we compared the expression of WDR5 by immunoblot in HeLa S3 and LNCaP cells and found them to be very similar (Figure S1D). To determine whether the WDR5-histone interaction is direct, we performed interaction assays using *in vitro* transcribed and translated radio-labeled WDR5 and biotinylated histone H3 peptides. *In vitro* translated WDR5 showed stronger binding with H3T11P peptide when compared to unmodified histone H3 peptide (Figure 1B). In agreement with published results, WDR5 also bound histone H3 dimethylated at lysine 4 peptide (Han et al., 2006; Wysocka et al., 2005) (Figure 1B). Similar results were obtained with bacterially-expressed and purified GST-WDR5 (Figure 1C). WDR5 interacted very weakly with H3T6P (histone H3 phosphorylated at threonine 6), and H3K9me3 tail peptides, while H3S10P (histone H3 phosphorylated at serine 10) enhanced binding of WDR5 (Figures S1E and S1F). We next asked whether other subunits of the WRAD module can also be retained on H3T11P peptide. Indeed, endogenous RBBP5 and ASH2L were also retained on H3T11P matrix (Figure 1D). As with H3T11P, H3K4me2 peptide also showed a similar retention profile. This interaction is likely mediated via WDR5, since *in vitro* radio-labeled RBBP5 and ASH2L did not directly interact with H3T11P peptide (Figure 1E).

For a better evaluation of these interactions at equilibrium, we measured the $K_d$ values of WDR5 for unmodified H3 or H3T11P peptides using isothermal titration calorimetry (ITC). Previous assays showed a wide range of $K_d$ values of WDR5-H3 tail interaction (Couture et

al., 2006; Trievel and Shilatifard, 2009). Our analysis showed that unmodified histone H3 peptide bound to WDR5 with a $K_d$ of 69 ± 16 μM (Figure S1G, left panel). We were not able to obtain higher measurement precision due to a relatively small ΔH of binding (-3.2 ± 0.9 kcal $mol^{-1}$) and relatively low concentration of WDR5 (close to $K_d$), since higher concentrations resulted in WDR5 precipitation. Nonetheless, the H3T11P peptide showed an approximately twofold increase in affinity, binding to WDR5 with a $K_d$ of 34 ± 15 μM (Figure S1G, right panel). This change in affinity is accompanied by a change in ΔH (-1.9 ± 0.4 kcal $mol^{-1}$), consistent with the possible involvement of a charged moiety in these interactions.

To determine WDR5 association with H3T11P in intact cells, we expressed FLAG-tagged WDR5 in LNCaP cells treated with or without AR agonist R1881, prepared soluble nuclear/nucleosomal fraction and subjected them to immunoprecipitation (IP) using anti-FLAG antibodies, followed by immunoblotting with anti-H3T11P antibodies. FLAG-WDR5 associated with endogenous H3T11P and such interactions were stimulated by R1881 treatment (Figure 1F). Taken together, these results demonstrate that WDR5 recognizes H3T11P with an approximately twofold higher affinity than unmodified histone H3 tail *in vitro*, and they raise the possibility that interactions between H3T11P and WDR5 may be important for recruitment of the SET1/MLL complex to AR target genes.

## Hormone sensitive recruitment and colocalization of WDR5 with H3T11P on AR target genes

Threonine 11 phosphorylation of histone H3 had been linked to transcriptional activation of AR target genes (Metzger et al., 2008). Since we observed interaction between WDR5 and H3T11P, we first analyzed whether WDR5 is critical for androgen-dependent genes activation using WDR5 knock-down LNCaP cells (Figure 2A and Tables S1 and S2). R1881 treatment led to higher expression levels of AR target genes in non-specific shRNA (shNS) LNCaP cells (Figure 2A, lanes 2 versus lanes 1 of each panel). Importantly, the mRNA levels of AR target genes decreased significantly in WDR5 knock-down cells treated with R1881 or dihydrotestosterone (DHT), the endogenous ligand of AR (Figure 2A and Figure S2A, lanes 4 and 6 versus lanes 2 of each panel). The depletion of WDR5 did not affect regulation of non-AR target genes, such as *PKIB* and *FOS*, in R1881 or DHT treated or untreated LNCaP cells, respectively (Figures S2B and S2C).

We next determined whether WDR5 is recruited to previously analyzed AR target genes and associates with H3T11P chromatin mark using chromatin immunoprecipitation (ChIP) and sequential ChIP (ChIP-reChIP) assays. We observed that H3T11P mark was enriched at the AREs of *KLK3*, *KLK2*, and *TMPRSS2* promoters/enhancers in R1881 or DHT treated LNCaP cells (Figure 2B and Figure S2D and Table S2). Importantly, we found that WDR5 recruitment to AR target genes was enhanced in R1881 or DHT stimulated cells (Figure 2C and Figure S2E). Furthermore, to determine whether H3T11P and WDR5 colocalize to the same chromatin regions, we performed ChIP-reChIP assays. Figure 2D shows that WDR5 and H3T11P co-occupied AR target genes in a ligand sensitive manner. We obtained similar results when the order of immunoprecipitations was reversed (Figure S3A). In addition to SET1/MLL complex, WDR5 is also found in host cell factor 1 (HCF-1), and ATAC and

NSL complexes, which contain acetyltransferases GCN5 and MOF, respectively (Cai et al., 2010; Dou et al., 2005; Lee et al., 2009; van Nuland et al., 2013; Wang et al., 2008; Wysocka et al., 2003). To determine whether any of these WDR5-containing chromatin modifying complexes are recruited to AR-responsive genes, we examined MLL4, GCN5, HCF-1, and MOF chromatin occupancy in R1881 treated cells. Here, we found that only MOF, but not MLL4, GCN5, and HCF-1 was consistently enriched to AR target genes following R1881 treatment (Figure 2E and Figures S3B-S3D). As a control, WDR5 and MOF occupancy, as well as H3T11P levels, did not change significantly on an androgen non-responsive *GAPDH* promoter after R1881 treatment (Figure S3E). Together these results demonstrate that WDR5 is recruited to and colocalizes with H3T11P marks on AR target genes in a hormone sensitive manner. Furthermore, these results suggest that WDR5-H3T11P association may facilitate recruitment of MOF to AR target genes.

## PKN1 activity is required for ligand-stimulated recruitment of WDR5 and the MLL1 complex to AR target genes

The kinase PKN1 is recruited to AR target genes upon R1881 stimulation leading to H3T11 phosphorylation (Metzger et al., 2008). To determine whether PKN1 is necessary for WDR5 recruitment and to further establish the importance of H3T11P in WDR5-mediated AR target genes regulation, we performed ChIP assays in PKN1 knock-down LNCaP cells treated with or without R1881 (Figure S4A and Table S1). Recruitment of PKN1 and AR, and the level of H3T11P increased on AR target genes in a ligand-dependent manner (Figure 3A and Figures S4B-S4E). PKN1 recruitment and H3T11 phosphorylation, upon PKN1 knock-down, were dampened (Figure 3A and Figures S4B and S4C), while the knock-down had no effect on AR occupancy (Figure 3A and Figure S4D). However, WDR5 recruitment was severely impaired on AR target genes in PKN1 knock-down cells (Figure 3B). To explore the possibility that the MLL1 complex is also recruited to AR target genes in a PKN1- and H3T11P-sensitive manner, we performed ChIP assays in PKN1 knock-down cells (Figure 3C and Figures S4F and S4G). MLL1, RBBP5, and ASH2L also associated with AR target genes upon R1881 treatment (Figure 3C and Figures S4F and S4G, lanes 2 versus lanes 1 of each panel). Importantly, knock-down of PKN1 severely interfered with the recruitment of the MLL1 complex to AR target genes (Figure 3C and Figures S4F and S4G, lanes 4 versus lanes 2 of each panel).

To determine whether phosphorylation of H3T11 and WDR5 recruitment require the enzymatic activity of PKN1, LNCaP cells treated with PKN1 inhibitor Ro318220 prior to and during R1881 stimulation were used in ChIP assays. PKN1 recruitment to chromatin was not impaired by Ro318220 treatment (Figure 3D and Figure S5A). Consistent with PKN1 knockdown, PKN1 inhibition decreased the level of H3T11P (Figure 3D and Figure S5B), but did not affect AR recruitment to target genes (Figure 3D and Figures S5C and S5D). However, PKN1 inhibitor treatment severely blocked recruitment of WDR5 and MLL1, RBBP5, and ASH2L to AR target genes in R1881 treated LNCaP cells (Figure 3E and 3F and Figure S5E and S5F). Together, these results demonstrate that PKN1 and its catalytic activity, and most likely H3T11P deposition, are required for hormone stimulated WDR5 and the MLL1 complex recruitment to AR target genes.

### PKN1/H3T11P-mediated recruitment of MLL1 complex to AR target genes leads to H3K4 methylation

To determine whether PKN1-mediated WDR5 and MLL1 complex recruitment has any functional consequence, we assessed H3K4 methylation levels at AR target genes by ChIP assays in PKN1 knock-down (Figures 4A and 4B) or PKN1 inhibitor-treated cells (Figures 4C and 4D). As expected, androgen stimulation significantly increased H3K4me2 and H3K4me3 levels in control knock-down cells (Figures 4A and 4B, lanes 2 versus lanes 1 of each panel). However, PKN1 depletion or inhibition abolished this change in both H3K4 di- and tri-methylation (Figures 4A-4D). The absence of H3K4 methylation is not due to overall histone loss as the level of total histone H3 did not change significantly (Figures S5G and S5H). Since MOF association with AR target genes enhanced upon ligand treatment (Figure 2E), and MOF acetylates histone H4 lysine 16 (Taipale et al., 2005), we performed ChIP assays for MOF recruitment, and H4K16 acetylation on AR target genes in PKN1 inhibitor treated cells. As expected, MOF occupancy and H4K16 acetylation were enriched at AR target genes in R1881 treated cells, but inhibition of PKN1 activity interfered with androgen induced recruitment of MOF and H4K16 acetylation on AR target genes (Figures 4E and 4F). These results are remarkably similar to our H3K4me2/3 findings and suggest that the H3T11P modification, likely through WDR5 recruitment, is critical for deposition of activating histone modifications on AR target genes.

### WDR5 is not necessary for recruitment of PKN1 and H3T11 phosphorylation

To test if there is a reciprocal relationship, we determined whether WDR5 is necessary for the recruitment of PKN1 and H3T11 phosphorylation at promoter/enhancer regions of AR target genes. WDR5 recruitment was significantly diminished in WDR5 knock-down cells treated with R1881 (Figure 5A). Since WDR5 is critical for SET1/MLL HMTase activity (Wysocka et al., 2005), ligand enhanced levels of H3K4me2 and H3K4me3 were also significantly down-regulated in WDR5 knock-down cells (Figures 5B and 5C). Importantly, WDR5 knock-down had little or no effect on recruitment of AR and PKN1 as well as the level of H3T11P in R1881-stimulated cells (Figures 5D-5F). These results indicate that PKN1 is necessary for chromatin association of WDR5 and H3K4 methylation, but WDR5 has no effect on ligand-stimulated AR and PKN1 recruitment, or H3T11 phosphorylation. Overall, our data implicate PKN1-mediated H3T11 phosphorylation as an entry point for WDR5 and MLL1 complex recruitment and subsequent H3K4 methylation.

### Genome-wide localization analysis of the H3T11P mark and WDR5

Having determined the co-occupancy of H3T11P marks and WDR5 on select AR target genes, we next wished to analyze their distributions throughout the genome. Using high throughput deep sequencing of chromatin immunoprecipitated DNA (ChIP-Seq) from LNCaP cells exposed to R1881 ligand or control solvent for 3 h, we generated genome-wide maps for the H3T11P mark and WDR5 occupancy. This 3 h treatment time was selected since it induced maximal binding based on our analysis of selected AR target genes (Figures 2B and 2C). Over 18 million clean reads were obtained for each chromatin IP from the sequencing run. Sequencing reads were aligned to the human reference genome and peak calling was performed. A Venn diagram depicting the number of occupied sites and the

overlap of WDR5 and H3T11P genomic binding/location sites in untreated or R1881 treated LNCaP cells is shown in Figure 6A. We found that while there were 2,612 H3T11P peaks, and only 833 WDR5 peaks in untreated cells, the number of peaks for both WDR5 and H3T11P increased significantly upon R1881 stimulation to 4,157 and 16,676 peaks, respectively. Importantly almost 41% of all WDR5 peaks colocalized with H3T11P peaks upon androgen stimulation, while only 1% H3T11P and WDR5 peaks overlapped in control cells. A plot of WDR5 and H3T11P ChIP-seq signal intensity relative to the center of WDR5 peaks showed significant overlap and androgen-induced enrichment of the H3T11P mark on WDR5-bound sites (Figure 6B).

Next, we analyzed the peak distribution profiles of the H3T11P mark and WDR5 relative to the positions of nearby genes. Unexpectedly, we found that upon hormone treatment there was a significant increase (from 2% to 23%) in H3T11P marks near promoters and 5'UTRs of annotated genes (Figure 6C). While the peak distribution pattern of WDR5 did not change substantially upon hormone treatment, the number of sites occupied by WDR5 increased remarkably (Figure 6D). Since the distribution of H3T11P marks on promoter and 5'UTRs of annotated genes showed a dramatic increase upon hormone treatment, we focused on analyzing these H3T11P marks overlapping with WDR5 near the promoter/5'UTR regions. Interestingly, we found that while there was only one colocalized peak in untreated cells, hormone treatment induced a remarkable 1,001 sites of H3T11P and WDR5 colocalization on annotated promoters/5'UTRs. Remarkably, 32% of all promoter/5'UTR H3T11P mark colocalized with WDR5 while 40% of all promoter/5'UTR-bound WDR5 localized with H3T11P marks in hormone treated cells (Figure 6E). Recently the mRNA-seq of R1881 treated LNCaP cells was reported (Tewari et al., 2012). Interestingly, only 339 genes were shown to be differentially expressed, out of which 202 genes were overexpressed upon hormone treatment (Tewari et al., 2012). Using this published data set in our analysis, we found that there was a substantial increase (from less than 1% to 21%) of H3T11P mark-WDR5 overlaps on these androgen responsive genes (Figure 6F). Similar results were obtained when all 339 androgen responsive genes (Figure S6A) or 164 genes (Figure S6B) that were shown to be common among 3 different gene expression studies (He et al., 2012; Massie et al., 2011; Tewari et al., 2012) were analyzed. Interestingly, while H3T11P marks and WDR5 binding were also observed on androgen repressed genes (137 genes total), their colocalization is less than what was observed for AR-activated genes (Figure S6C). Based on our ChIP-seq data, we selected two additional androgen responsive genes for confirmation by conventional ChIP-qPCR. WDR5 and H3T11P were enriched on the *IGF2R* and *RPL13A* androgen-responsive gene promoters, sites also occupied by AR (based on previously published AR ChIP-seq data (Yu et al., 2010)) (Figure 6G and Figure S6D). Additionally, WDR5 was hyper-recruited and H3T11P marks were enhanced on the promoters of these two genes as determined by ChIP-qPCR (Figure 6H and Figure S6E). Accordingly, knock-down of WDR5 attenuated expression of these two androgen responsive genes (Figure 6I and Figures S6F and S6G). Together these ChIP-seq data are in agreement with previous gene specific studies and establish a functional interaction between H3T11P marks and WDR5 localization at a genome wide level.

### WDR5 promotes prostate cancer cell proliferation and is overexpressed in human prostate cancers

Having demonstrated that WDR5 is enriched at the promoter/enhancer regions of AR target genes in R1881 treated cells and is necessary for AR function; we next investigated whether WDR5 plays a role in R1881 stimulated LNCaP cell proliferation. In the absence of androgen, LNCaP cells proliferated very slowly; however, proliferation was significantly stimulated by R1881 treatment (Figures 7A and 7B). Both BrdU and alamarBlue assays indicated markedly decreased proliferation rates in R1881 treated cells upon WDR5 depletion when compared to control knock-down cells (Figures 7A and 7B, respectively). As expected, WDR5 overexpression in LNCaP cells only slightly enhanced proliferation of cells under hormone treated condition (Figure S7A), and WDR5 knock-down had minimal effect on growth of the AR negative RWPE-1 (normal prostate epithelial cell line) and PC-3 (prostate cancer cells) (Figures S7B and S7C). These results demonstrate a growth promoting role of WDR5 in hormone stimulated proliferation of prostate cancer cells.

The strict requirements for WDR5 in hormone-stimulated LNCaP cell proliferation and the previously reported enhanced H3T11P staining in human prostate cancers (Metzger et al., 2008) prompted us to ask if WDR5 expression is also increased in human prostate cancers. We, therefore, examined WDR5 expression in a large cohort of human prostate cancer samples using immunohistochemical analysis of tissue microarrays. We found that normal prostate acina epithelial cells had very low immunoreactivity for WDR5. In contrast, prostate cancer cells had strong and diffuse immunoreactivity for WDR5 (Figure 7C). In prostate cancer cells, WDR5 protein was detected in both the nucleus and the cytoplasm. Semi-quantitative analysis showed that prostate cancer had significantly higher immunoreactivity for WDR5 than normal epithelial cells of the prostatic acini ($p < 0.001$) (Figures 7C and 7D). Further analysis revealed that nuclear and cytoplasmic WDR5 expression was significantly higher in all stages (and Gleason scores of 3-5) of prostate cancer when compared to normal tissues (Figures 7D-7F). In prostate cancer, WDR5 expression did not correlate with different tumor grades and stages, indicating WDR5 overexpression is an early genetic event for prostate cancer development (Figures 7E and 7F). Collectively, these data strongly suggest that WDR5 plays an important role in prostate cancer cell proliferation and its upregulation may contribute to prostate tumorigenesis.

## DISCUSSION

In this work, we identified WDR5 as a potential transducer protein of phospho-H3T11 mark and demonstrated the importance of this interaction for MLL1 complex and MOF recruitment and subsequent histone H3K4 methylation and H4K16 acetylation. At the genome-wide level, we found significant colocalization of WDR5 and H3T11P in androgen-treated cells. Finally, we demonstrated that WDR5 is critical for cell proliferation and is upregulated in human prostate cancers. Thus, this work identifies WDR5 as a key mediator of H3T11P chromatin mark in the context of androgen-dependent transcriptional regulation and prostate cancer.

H3T11 phosphorylation by PKN1 has been reported to accelerate demethylation of H3K9 via KDM4C and KDM1A histone lysine demethylases (Metzger et al., 2008). Additionally,

PKM2-mediated H3T11 phosphorylation releases HDAC3 from chromatin, enabling subsequent histone acetylation (Yang et al., 2012). In all cases, the current literature suggests that H3T11P functions in the context of prevention of removal of activating mark or promotion of repressing marks. Our findings now suggest H3T11P also serves as a signal for recruitment of positively activating histone modifying activities including MLL1 complex and MOF. Interestingly, it was previously shown that MLL1 complex coordinates with MOF in activating target gene expression through H3K4 methylation and H4K16 acetylation, and MOF plays a role in WDR5 recruitment and H3K4 methylation in stem cells (Dou et al., 2005; Li et al., 2012). Based on our studies, it is tempting to propose a stepwise mechanism in which PKN1 recruitment and H3T11P precede WDR5 chromatin occupancy and H3K4 methylation and H4K16 acetylation during gene activation in androgen-stimulated cells (Figure 7G). However, it is also possible that stable WDR5 recruitment and retention to the transcription complex is simply dependent on PKN1. However, genome-wide colocalization studies under PKN1 knock-down or inhibition will be necessary to determine the mature of this proposed mechanism. Nonetheless, our results together with those from Metzger et al. (Metzger et al., 2008) show that H3T11P plays an anchoring role in recruitment of proteins and enzymatic complexes that establish activating marks on and remove repressing marks from AR target genes.

We wonder whether WDR5, by virtue of its ability to associate with H3T11P and H3K4me2, facilitates a better substrate presentation to the enzymatic subunit of the MLL1 complex, for histone H3K4 trimethylation leading to gene activation. Interestingly, in the crystal structure of WDR5 bound to histone peptides, histone H3 arginine 2, and threonine 3 residues, make extensive contacts with WDR5 (Couture et al., 2006; Han et al., 2006; Ruthenburg et al., 2006). While H3K4 does not show any direct interaction with WDR5 residues, it was suggested that WDR5 interaction with histone H3 allows proper presentation of H3K4 for methylation by MLL1 complex (Ruthenburg et al., 2006). Unfortunately, none of the peptides used in the crystal structure analyses included threonine 11, making it difficult to test our current predictions. Although *in vitro* ITC data show a modest twofold increase in affinity of WDR5 for H3T11P, our numerous assays in intact cells demonstrate the physiologic relevance of the interaction. These *in vitro* and *in vivo* results when analyzed in a biological context suggest that H3T11 phosphorylation has a modulatory or facilitatory role in WDR5 binding to histones and targeting to transcriptional regulatory regions. While phosphorylation of histone H3 threonine 3 has negative effect on WDR5 binding (Couture et al., 2006) and H3T6P did not have any appreciable effect on WDR5 binding, H3S10P peptides retained WDR5. Because H3S10P has not been studied in the context of androgen signaling, we did not pursue any further characterization of this interaction. We, however, note that since H3S10P has been linked to activation of immediate early genes (Banerjee and Chakravarti, 2011; Duncan et al., 2006; Macdonald et al., 2005; Soloaga et al., 2003; Zippo et al., 2007), it is possible that H3S10P-WDR5 interaction may have a role in activation of these immediate early genes. Finally, a previous report also showed that the WDR5 histone binding motif is also the MLL interaction motif (Song and Kingston, 2008). Therefore, it appears that WDR5 may contact multiple partners, and multiple sites some of which may still be undiscovered, through an elaborate binding profile to regulate transcription. Consistent with this, a recent report showed that WDR5 in addition to binding

to histone tail (a.a 1-10) also independently interact with histone H3 residues 10-31 (Kim et al., 2013).

PKN1 dependent and H3T11P-mediated WDR5 recruitment may act to link MLL1 complex to activated nuclear receptors in order to increase target gene expression via histone H3K4 methylation. This process, thus, ensures that androgen-dependent PKN1 recruitment is integrated into a functional and positive transcriptional outcome. In this context, our genome-wide binding studies shed important and novel information. First, we observed a significant enrichment of H3T11P near the promoters of annotated genes suggesting, for the first time, that H3 threonine 11 phosphorylation may be a common property for genes that utilize this mark. Second, we found that a large number of androgen responsive genes are co-occupied by H3T11P and WDR5 suggesting a functional link between this histone modification and WDR5. Third, we found that almost half of WDR5 peaks colocalized with H3T11P peaks. However, our results also identified H3T11P peaks and WDR5 peaks that did not overlap. These results raise the possibility that H3T11P chromatin signaling involves mechanisms that are both dependent and independent of WDR5. Similarly, mechanisms not involving H3T11P may also contribute to WDR5 chromatin targeting. Future studies will determine whether the WDR5-H3T11P interaction is a general mechanism of transcriptional activation mediated by other members of the nuclear receptor superfamily and other activated transcriptional signaling pathways.

We observed a robust effect of WDR5 knock-down on androgen-stimulated prostate cancer cell proliferation. Moreover, the remarkable differences in WDR5 expression that we detected between normal and prostate cancer tissue samples strongly implies that WDR5 overexpression may play a role in prostate cancer initiation. Previously, the Schüle laboratory showed a significant increase in H3T11P and H3K4 methylation marks in human prostate cancers (Metzger et al., 2010; Metzger et al., 2008). We suggest that hyperexpression of WDR5 is necessary to propagate an increased H3T11P signal in prostate cancers. In prostate cancers, enhanced interaction between WDR5 and H3T11P leads to recruitment of the MLL1 complex to chromatin, resulting in hypermethylation of H3K4. Activation of this signaling cascade promotes AR dependent genes activation and enhanced or abnormal proliferation of cells and prostate tumorigenesis (Figure 7G). Consistent with this hypothesis, WDR5 and MOF have recently been reported as critical factors in the maintenance of ES cell pluripotency and self-renewal by increasing H3K4 methylation and H4K16 acetylation in ESCs (Ang et al., 2011; Li et al., 2012). Furthermore, the SET/MLL complex is essential for survival and proliferation during early embryogenesis (Tyagi et al., 2007). Our results indicate that the expression of WDR5 may be a key initiating event in prostate tumorigenesis. It remains to be seen whether upregulation of WDR5 expression and H3T11P and H3K4me levels are common signatures of other hormone sensitive human cancers.

In summary, we have uncovered a mechanism involving a successive series of signaling events by PKN1–H3T11P–WDR5–H3K4me3 that lead to AR target gene activation. PKN1 dependent MOF recruitment possibly via WDR5 and subsequent H4K16 acetylation, also highlights a role for H3T11P in recruitment of positively acting histone modifying activities to target promoters. Our findings demonstrate a key role for WDR5 in cell proliferation, and

we wonder whether WDR5 expression could be used as a prognostic marker for detecting initial stages of prostate cancer and whether low molecular weight compound blocking H3T11P-WDR5 interaction may have therapeutic potential in prostate cancers.

## EXPRIMENTAL PROCEDURES

### Cell culture and treatment

LNCaP cells were hormone-starved for 2 days and treated with 10 nM R1881 or 10 nM DHT for 16 h (for expression assay), or for 3 h (for ChIP assays). For assay involving PKN1 inhibitor, cells were cultivated for 30 min in the presence or absence of 10 μM PKN1 inhibitor, Ro318220 prior to R1881 addition.

### Histone peptide pull down assays and protein identification by MS

HeLa S3 nuclear extracts were incubated with biotinylated and modified or unmodified histone H3 peptides. The bound proteins were eluted and sequenced by MALDI-TOF MS/MS analysis (Alphalyse, California, USA).

### Protein interaction assay

*In vitro* transcribed and translated [$^{35}$S]-labeled WDR5 (for protein interaction assay) or purified GST-WDR5 (for GST-pull down assay), or LNCaP nuclear extracts (for endogenous protein interaction assay) were incubated with biotinylated histone H3 peptides. The pulled-down proteins were analyzed by phosphoimager or immunoblot.

### Nuclear/nucleosomal protein preparation

Nuclear protein extraction was performed as previously described, with minor modifications (Parker et al., 2012).

### ChIP assays and sequential ChIP

ChIP assay was performed essentially as previously described, with minor modifications (Parker et al., 2012). For sequential ChIP (ChIP-reChIP), first-round ChIPs were performed as previously described (Parker et al., 2012) except that following the final wash, and beads were resuspended in elution buffer. WDR5 and H3T11P ChIP eluates were again subjected to ChIP (reChIP) with anti-H3T11P or anti-WDR5 antibodies, respectively. Determination of relative enrichment was performed by qPCR. The primer sequences are provided in Table S2.

### ChIP-sequencing and data analysis

Barcoded sequencing libraries were generated using KAPA Library Preparation Kits (Kapa Biosystems, Massachusetts, USA) according to the manufacturer's protocol, beginning with 2 ng of ChIP DNA or input chromatin-derived DNA from LNCaP cells. Analysis was performed as described previously (Barish et al., 2012), with slight modifications. Sequencing data files were aligned to the hg18 human reference genome using Bowtie (version 0.12.9) and standard parameters. Peak calling and analysis was performed using HOMER, the methods of which are freely available at http://biowhat.ucsd.edu/homer/. Only

unique sequencing tags were considered for analysis. Results were visualized by preparing custom tracks for the UCSC browser. Peaks were identified using a false discovery rate of < 0.1%, and input chromatin-derived DNAs from ethanol or R1881-treated cells were used as controls. Identified peaks were annotated to the nearest transcription start site. Colocalizaton between WDR5 and H3T11P was determined using a 500 base pair window between the centers of identified peaks. ChIP fragment depth was calculated by extending sequencing tags by their estimated ChIP fragment lengths.

### BrdU and AlamarBlue Cell proliferation assay

Control and WDR5 knock-down LNCaP cells were seeded at 5,000 per well in 48-well tissue culture plates. After 24 h treatment of ethanol or R1881, cells were incubated in a medium containing BrdU or alamarBlue for 2 h and fluorescence was measured. This represents day 1 of the assay. This process was repeated every 24 h for 4 consecutive days.

### Immunohistochemistry and TMAs

TMAs contained 8 normal prostate tissue, and 71 prostate cancer samples. TMA slides were immunohistochemical stained and were blindly evaluated by a pathologist using a semi-quantitative dual-scoring system as described previously (Wei et al., 2006).

### Statistical analysis

Data are expressed as the means and standard deviations (SDs) of three independent experiments. Statistical significance ($P<0.05$) was evaluated by the Student's 2-tailed t-test.

### Deposition of ChIP-seq data

The raw ChIP-seq data-set is being submitted to Gene Expression Omnibus.

## Supplementary Material

Refer to Web version on PubMed Central for supplementary material.

## Acknowledgments

We thank Winship Herr for generously providing a rabbit polyclonal WDR5 antibody. Work in the D.C laboratory is supported in part by NIH RO1 CA133755, PO1 HD 57877, and institutional (Robert H. Lurie Comprehensive Cancer Center and NU) grants and support. We thank Ms. Nandini Chattopadhyay for technical assistance.

## REFERENCES

Ang YS, Tsai SY, Lee DF, Monk J, Su J, Ratnakumar K, Ding J, Ge Y, Darr H, Chang B, et al. Wdr5 mediates self-renewal and reprogramming via the embryonic stem cell core transcriptional network. Cell. 2011; 145:183–197. [PubMed: 21477851]

Banerjee T, Chakravarti D. A peek into the complex realm of histone phosphorylation. Mol. Cell. Biol. 2011; 31:4858–4873. [PubMed: 22006017]

Bannister AJ, Kouzarides T. Regulation of chromatin by histone modifications. Cell Res. 2011; 21:381–395. [PubMed: 21321607]

Barish GD, Yu RT, Karunasiri MS, Becerra D, Kim J, Tseng TW, Tai LJ, Leblanc M, Diehl C, Cerchietti L, et al. The Bcl6-SMRT/NCoR cistrome represses inflammation to attenuate atherosclerosis. Cell Metab. 2012; 15:554–562. [PubMed: 22465074]

Cai Y, Jin J, Swanson SK, Cole MD, Choi SH, Florens L, Washburn MP, Conaway JW, Conaway RC. Subunit composition and substrate specificity of a MOF-containing histone acetyltransferase distinct from the male-specific lethal (MSL) complex. J. Biol. Chem. 2010; 285:4268–4272. [PubMed: 20018852]

Calo E, Wysocka J. Modification of enhancer chromatin: what, how, and why? Mol. Cell. 2013; 49:825–837. [PubMed: 23473601]

Campos EI, Reinberg D. Histones: annotating chromatin. Annu. Rev. Genet. 2009; 43:559–599. [PubMed: 19886812]

Chi P, Allis CD, Wang GG. Covalent histone modifications--miswritten, misinterpreted and mis-erased in human cancers. Nat. Rev. Cancer. 2010; 10:457–469. [PubMed: 20574448]

Couture JF, Collazo E, Trievel RC. Molecular recognition of histone H3 by the WD40 protein WDR5. Nat. Struct. Mol. Biol. 2006; 13:698–703. [PubMed: 16829960]

Dasgupta S, Lonard DM, O'Malley BW. Nuclear Receptor Coactivators: Master Regulators of Human Health and Disease. Annu. Rev. Med. 2014; 14:279–292. [PubMed: 24111892]

Dou Y, Milne TA, Ruthenburg AJ, Lee S, Lee JW, Verdine GL, Allis CD, Roeder RG. Regulation of MLL1 H3K4 methyltransferase activity by its core components. Nat. Struct. Mol. Biol. 2006; 13:713–719. [PubMed: 16878130]

Dou Y, Milne TA, Tackett AJ, Smith ER, Fukuda A, Wysocka J, Allis CD, Chait BT, Hess JL, Roeder RG. Physical association and coordinate function of the H3 K4 methyltransferase MLL1 and the H4 K16 acetyltransferase MOF. Cell. 2005; 121:873–885. [PubMed: 15960975]

Duncan EA, Anest V, Cogswell P, Baldwin AS. The kinases MSK1 and MSK2 are required for epidermal growth factor-induced, but not tumor necrosis factor-induced, histone H3 Ser10 phosphorylation. J. Biol. Chem. 2006; 281:12521–12525. [PubMed: 16517600]

Eissenberg JC, Shilatifard A. Histone H3 lysine 4 (H3K4) methylation in development and differentiation. Dev. Biol. 2010; 339:240–249. [PubMed: 19703438]

Han Z, Guo L, Wang H, Shen Y, Deng XW, Chai J. Structural basis for the specific recognition of methylated histone H3 lysine 4 by the WD-40 protein WDR5. Mol. Cell. 2006; 22:137–144. [PubMed: 16600877]

He HH, Meyer CA, Chen MW, Jordan VC, Brown M, Liu XS. Differential DNase I hypersensitivity reveals factor-dependent chromatin dynamics. Genome Res. 2012; 22:1015–1025. [PubMed: 22508765]

Izumi K, Mizokami A, Lin WJ, Lai KP, Chang C. Androgen receptor roles in the development of benign prostate hyperplasia. Am. J. Pathol. 2013; 182:1942–1949. [PubMed: 23570837]

Kim DH, Tang Z, Shimada M, Fierz B, Houck-Loomis B, Bar-Dagen M, Lee S, Lee SK, Muir TW, Roeder RG, et al. Histone H3K27 trimethylation inhibits H3 binding and function of SET1-like H3K4 methyltransferase complexes. Mol. Cell. Biol. 2013; 33:4936–4946. [PubMed: 24126056]

Lee S, Roeder RG, Lee JW. Roles of histone H3-lysine 4 methyltransferase complexes in NR-mediated gene transcription. PNAS. 2009; 87:343–382.

Li X, Li L, Pandey R, Byun JS, Gardner K, Qin Z, Dou Y. The histone acetyltransferase MOF is a key regulator of the embryonic stem cell core transcriptional network. Cell Stem Cell. 2012; 11:163–178. [PubMed: 22862943]

Loomis RJ, Naoe Y, Parker JB, Savic V, Bozovsky MR, Macfarlan T, Manley JL, Chakravarti D. Chromatin binding of SRp20 and ASF/SF2 and dissociation from mitotic chromosomes is modulated by histone H3 serine 10 phosphorylation. Mol. Cell. 2009; 33:450–461. [PubMed: 19250906]

Macdonald N, Welburn JP, Noble ME, Nguyen A, Yaffe MB, Clynes D, Moggs JG, Orphanides G, Thomson S, Edmunds JW, et al. Molecular basis for the recognition of phosphorylated and phosphoacetylated histone h3 by 14-3-3. Mol. Cell. 2005; 20:199–211. [PubMed: 16246723]

Massie CE, Lynch A, Ramos-Montoya A, Boren J, Stark R, Fazli L, Warren A, Scott H, Madhu B, Sharma N, et al. The androgen receptor fuels prostate cancer by regulating central metabolism and biosynthesis. EMBO J. 2011; 30:2719–2733. [PubMed: 21602788]

Metzger E, Imhof A, Patel D, Kahl P, Hoffmeyer K, Friedrichs N, Muller JM, Greschik H, Kirfel J, Ji S, et al. Phosphorylation of histone H3T6 by PKCbeta(I) controls demethylation at histone H3K4. Nature. 2010; 464:792–796. [PubMed: 20228790]

Metzger E, Yin N, Wissmann M, Kunowska N, Fischer K, Friedrichs N, Patnaik D, Higgins JM, Potier N, Scheidtmann KH, et al. Phosphorylation of histone H3 at threonine 11 establishes a novel chromatin mark for transcriptional regulation. Nat. Cell Biol. 2008; 10:53–60. [PubMed: 18066052]

Musselman CA, Lalonde ME, Cote J, Kutateladze TG. Perceiving the epigenetic landscape through histone readers. Nat. Struct. Mol. Biol. 2012; 19:1218–1227. [PubMed: 23211769]

Nowak SJ, Corces VG. Phosphorylation of histone H3: a balancing act between chromosome condensation and transcriptional activation. Trends Genet. 2004; 20:214–220. [PubMed: 15041176]

Parker JB, Palchaudhuri S, Yin H, Wei J, Chakravarti D. A transcriptional regulatory role of the THAP11-HCF-1 complex in colon cancer cell function. Mol. Cell. Biol. 2012; 32:1654–1670. [PubMed: 22371484]

Patel A, Vought VE, Dharmarajan V, Cosgrove MS. A conserved arginine-containing motif crucial for the assembly and enzymatic activity of the mixed lineage leukemia protein-1 core complex. J. Biol. Chem. 2008; 283:32162–32175. [PubMed: 18829457]

Perissi V, Jepsen K, Glass CK, Rosenfeld MG. Deconstructing repression: evolving models of co-repressor action. Nat. Rev. Genet. 2010; 11:109–123. [PubMed: 20084085]

Preuss U, Landsberg G, Scheidtmann KH. Novel mitosis-specific phosphorylation of histone H3 at Thr11 mediated by Dlk/ZIP kinase. Nucleic acids Res. 2003; 31:878–885. [PubMed: 12560483]

Rosenfeld MG, Glass CK. Coregulator codes of transcriptional regulation by nuclear receptors. J. Biol. Chem. 2001; 276:36865–36868. [PubMed: 11459854]

Ruthenburg AJ, Wang W, Graybosch DM, Li H, Allis CD, Patel DJ, Verdine GL. Histone H3 recognition and presentation by the WDR5 module of the MLL1 complex. Nat. Struct. Mol. Biol. 2006; 13:704–712. [PubMed: 16829959]

Schrecengost R, Knudsen KE. Molecular pathogenesis and progression of prostate cancer. Semin. Oncol. 2013; 40:244–258. [PubMed: 23806491]

Shafi AA, Yen AE, Weigel NL. Androgen receptors in hormone-dependent and castration-resistant prostate cancer. Pharmacol. Ther. 2013; 140:223–238. [PubMed: 23859952]

Shang Y, Myers M, Brown M. Formation of the androgen receptor transcription complex. Mol. Cell. 2002; 9:601–610. [PubMed: 11931767]

Shilatifard A. The COMPASS family of histone H3K4 methylases: mechanisms of regulation in development and disease pathogenesis. Annu. Rev. Biochem. 2012; 81:65–95. [PubMed: 22663077]

Shimada M, Niida H, Zineldeen DH, Tagami H, Tanaka M, Saito H, Nakanishi M. Chk1 is a histone H3 threonine 11 kinase that regulates DNA damage-induced transcriptional repression. Cell. 2008; 132:221–232. [PubMed: 18243098]

Soloaga A, Thomson S, Wiggin GR, Rampersaud N, Dyson MH, Hazzalin CA, Mahadevan LC, Arthur JS. MSK2 and MSK1 mediate the mitogen- and stress-induced phosphorylation of histone H3 and HMG-14. EMBO J. 2003; 22:2788–2797. [PubMed: 12773393]

Song JJ, Kingston RE. WDR5 interacts with mixed lineage leukemia (MLL) protein via the histone H3-binding pocket. J. Biol. Chem. 2008; 283:35258–35264. [PubMed: 18840606]

Steward MM, Lee JS, O'Donovan A, Wyatt M, Bernstein BE, Shilatifard A. Molecular regulation of H3K4 trimethylation by ASH2L, a shared subunit of MLL complexes. Nat. Struct. Mol. Biol. 2006; 13:852–854. [PubMed: 16892064]

Suganuma T, Workman JL. Signals and combinatorial functions of histone modifications. Annu. Rev. Biochem. 2011; 80:473–499. [PubMed: 21529160]

Taipale M, Rea S, Richter K, Vilar A, Lichter P, Imhof A, Akhtar A. hMOF histone acetyltransferase is required for histone H4 lysine 16 acetylation in mammalian cells. Mol. Cell. Biol. 2005; 25:6798–6810. [PubMed: 16024812]

Takayama K, Inoue S. Transcriptional network of androgen receptor in prostate cancer progression. Int. J. Urol. 2013; 20:756–768. [PubMed: 23600948]

Tewari AK, Yardimci GG, Shibata Y, Sheffield NC, Song L, Taylor BS, Georgiev SG, Coetzee GA, Ohler U, Furey TS, et al. Chromatin accessibility reveals insights into androgen receptor activation and transcriptional specificity. Genome Biol. 2012; 13:R88. [PubMed: 23034120]

Trievel RC, Shilatifard A. WDR5, a complexed protein. Nat. Struct. Mol. Biol. 2009; 16:678–680. [PubMed: 19578375]

Tyagi S, Chabes AL, Wysocka J, Herr W. E2F activation of S phase promoters via association with HCF-1 and the MLL family of histone H3K4 methyltransferases. Mol. Cell. 2007; 27:107–119. [PubMed: 17612494]

van Nuland R, Smits AH, Pallaki P, Jansen PW, Vermeulen M, Timmers HT. Quantitative dissection and stoichiometry determination of the human SET1/MLL histone methyltransferase complexes. Mol. Cell. Biol. 2013; 33:2067–2077. [PubMed: 23508102]

Wang YL, Faiola F, Xu M, Pan S, Martinez E. Human ATAC Is a GCN5/PCAF-containing acetylase complex with a novel NC2-like histone fold module that interacts with the TATA-binding protein. J. Biol. Chem. 2008; 283:33808–33815. [PubMed: 18838386]

Wei JJ, Chiriboga L, Arslan AA, Melamed J, Yee H, Mittal K. Ethnic differences in expression of the dysregulated proteins in uterine leiomyomata. Human Rep. 2006; 21:57–67.

Wissmann M, Yin N, Muller JM, Greschik H, Fodor BD, Jenuwein T, Vogler C, Schneider R, Gunther T, Buettner R, et al. Cooperative demethylation by JMJD2C and LSD1 promotes androgen receptor-dependent gene expression. Nat. Cell Biol. 2007; 9:347–353. [PubMed: 17277772]

Wysocka J, Myers MP, Laherty CD, Eisenman RN, Herr W. Human Sin3 deacetylase and trithorax-related Set1/Ash2 histone H3-K4 methyltransferase are tethered together selectively by the cell-proliferation factor HCF-1. Genes Dev. 2003; 17:896–911. [PubMed: 12670868]

Wysocka J, Swigut T, Milne TA, Dou Y, Zhang X, Burlingame AL, Roeder RG, Brivanlou AH, Allis CD. WDR5 associates with histone H3 methylated at K4 and is essential for H3 K4 methylation and vertebrate development. Cell. 2005; 121:859–872. [PubMed: 15960974]

Yang W, Xia Y, Hawke D, Li X, Liang J, Xing D, Aldape K, Hunter T, Alfred Yung WK, Lu Z. PKM2 phosphorylates histone H3 and promotes gene transcription and tumorigenesis. Cell. 2012; 150:685–696. [PubMed: 22901803]

Yu J, Mani RS, Cao Q, Brenner CJ, Cao X, Wang X, Wu L, Li J, Hu M, Gong Y, et al. An integrated network of androgen receptor, polycomb, and TMPRSS2-ERG gene fusions in prostate cancer progression. Cancer cell. 2010; 17:443–454. [PubMed: 20478527]

Zippo A, De Robertis A, Serafini R, Oliviero S. PIM1-dependent phosphorylation of histone H3 at serine 10 is required for MYC-dependent transcriptional activation and oncogenic transformation. Nat. Cell Biol. 2007; 9:932–944. [PubMed: 17643117]

## HIGHLIGHTS

1. H3T11P facilitates WDR5 and MLL1 complex recruitment
2. Genome wide localization of WDR5 and H3T11P analyzed
3. A mechanism involving WDR5 and H3T11P in AR target gene activation is established
4. WDR5 is overexpressed in prostate cancer and critical for cancer cell proliferation

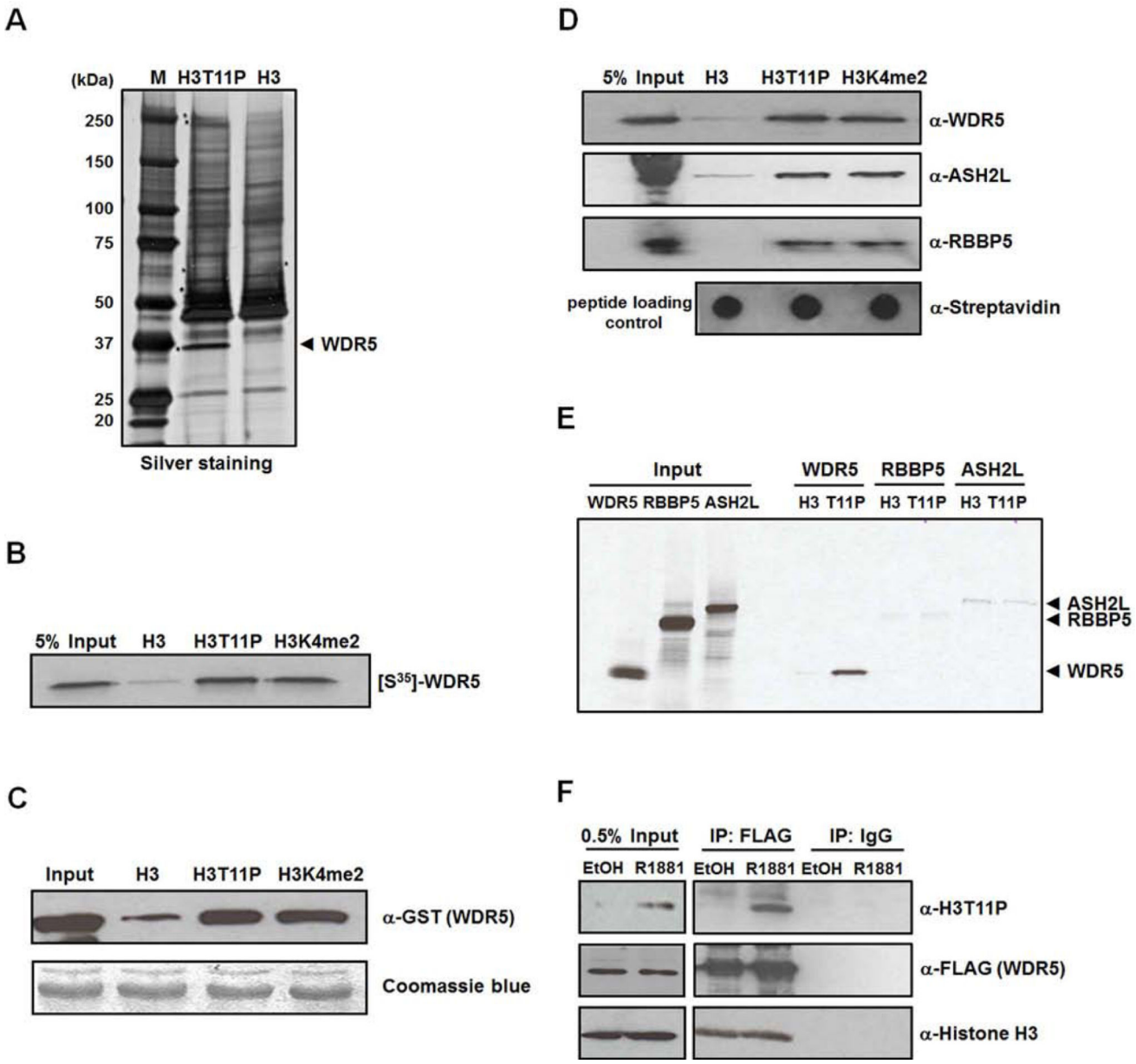


**Figure 1. WDR5 interacts with threonine 11 phosphorylated histone H3**

(A) Unmodified histone H3 and H3T11P peptide binding proteins were purified from HeLa S3 nuclear extracts. Differentially bound proteins were detected with silver staining and identified by MALDI-TOF MS/MS analysis. One of the bound proteins was identified as WDR5. (B) pCMX-WDR5 was *in vitro* transcribed and translated and incubated with indicated histone H3 peptides conjugated with biotin. Streptavidin-pulled-down proteins were analyzed by phosphorimager. (C) Biotinylated histone H3 peptides containing indicated modifications were incubated with purified GST-WDR5. Streptavidin-pulled-down proteins were immunoblotted with anti-GST antibody. (D) LNCaP nuclear extracts were incubated with indicated biotinylated histone H3 peptides. Pulled-down proteins were analyzed by immunoblotting using indicated antibodies. Peptide loading controls were detected using anti-streptavidin antibody. (E) pCMXWDR5, pCMX-RBBP5 or pCMX-

ASH2L was *in vitro* transcribed and translated and incubated with biotinylated histone H3 or H3T11P peptides. Pulled-down proteins were analyzed by phosphorimager. (F) LNCaP soluble nuclear/nucleosomal extracts expressing FLAG-tagged WDR5 were immunoprecipitated with indicated antibodies, and the immunoprecipitates were immunoblotted wirh H3T11P, FLAG (WDR5), and histone H3 antibodies. See also Figure S1.

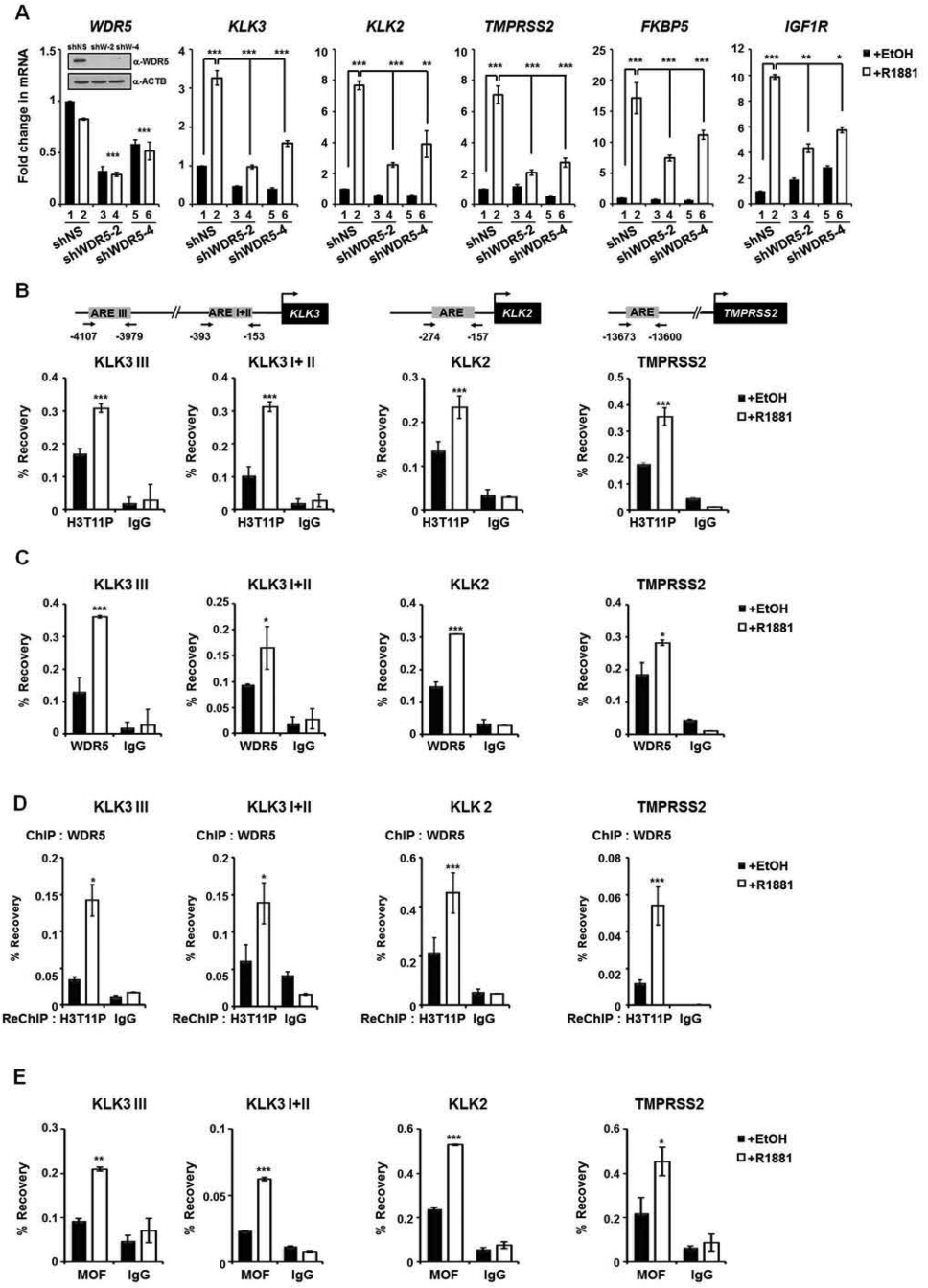


**Figure 2. WDR5 regulates androgen signaling and co-associates with H3T11P on AR target genes**

(A) Control (shNS) or WDR5 knock-down LNCaP cells were grown in the presence or absence of R1881 and mRNA levels of AR target genes and *WDR5* were analyzed by qRT-PCR. (B-E) Schematic diagram of amplicons flanking AREs in the promoter/enhancer regions of *KLK3*, *KLK2*, and *TMPRSS2* genes (upper panel). ChIP assays at the AR target genes in R1881-treated or untreated LNCaP cells were conducted using anti-H3T11P (B), anti-WDR5 (C) or control IgG antibodies and examined by qPCR. (D) Sequential ChIP

assays of androgen-stimulated LNCaP cells at AR target genes. WDR5 ChIP followed by H3T11P or control IgG re-ChIP. (E) ChIP assays at the AR target genes using anti-MOF or control antibodies in with or without R1881 LNCaP cells. Values represent the mean ± standard deviation of duplicated qPCRs from a representative experiment. Experiments were performed three times with similar results. *$p < 0.05$; **$p < 0.01$; ***$p< 0.001$. See also Figures S2 and S3 and Tables S1 and S2.

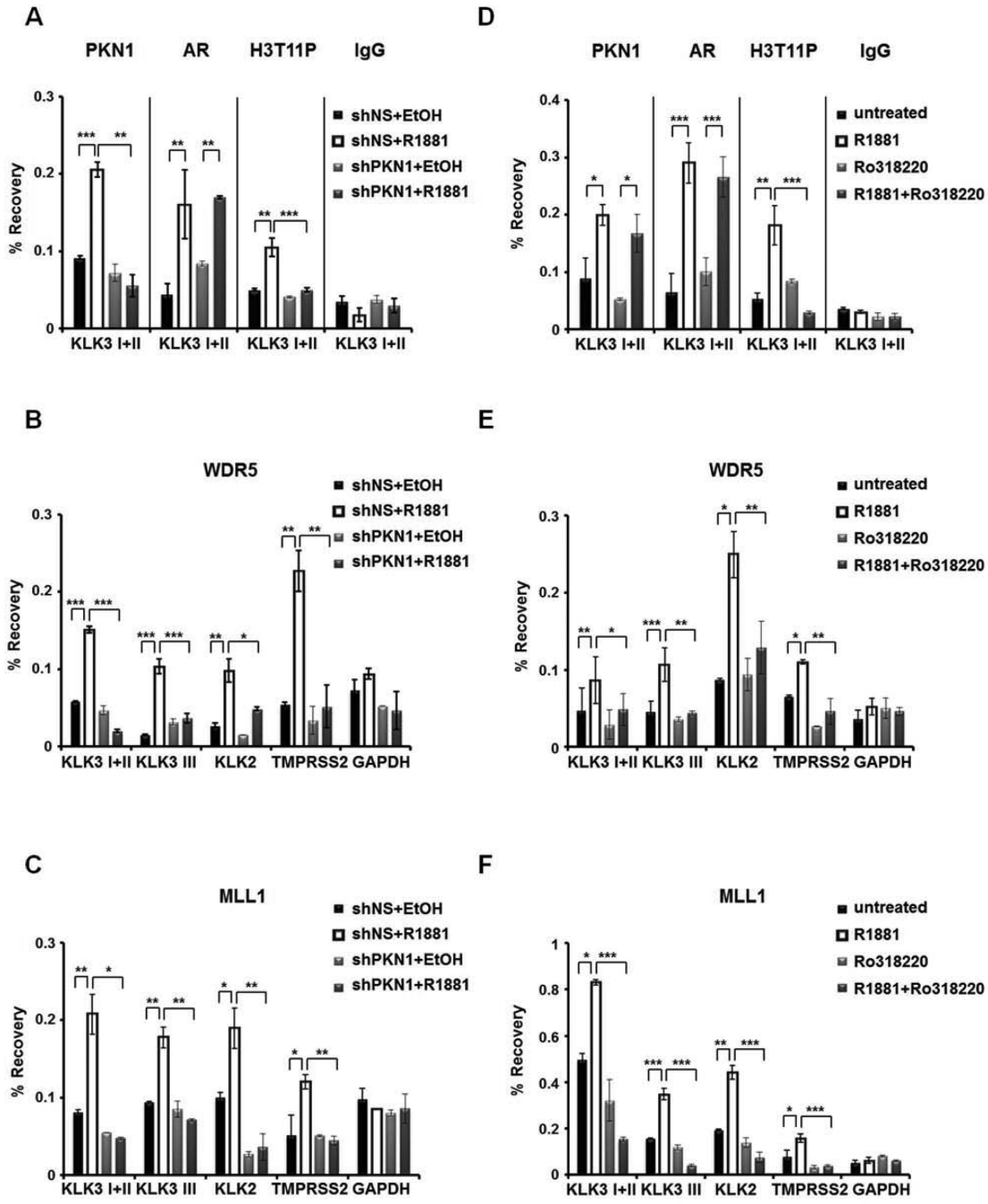


**Figure 3. PKN1 regulates the recruitment of WDR5 and MLL1 complex to AR target genes**

(A-C) Control (shNS) or PKN1 knock-down LNCaP cells were cultivated in the presence or absence of R1881. (D-F) LNCaP cells were grown in the presence or absence of the PKN1 inhibitor Ro318220 prior to and during R1881 stimulation. (A and D) ChIP was performed using indicated antibodies. The precipitated chromatin was amplified by qPCR using primers flanking ARE in the promoter region of the *KLK3* gene. (B, C, E, and F) ChIP assays were performed with the WDR5 (B and E), and MLL1 (C and F) antibodies at AR target genes. Values represent the mean ± standard deviation of duplicated qPCRs from a

representative experiment. Experiments were performed three times with similar results. *p < 0.05; **p < 0.01; ***p< 0.001. See also Figures S4 and S5.

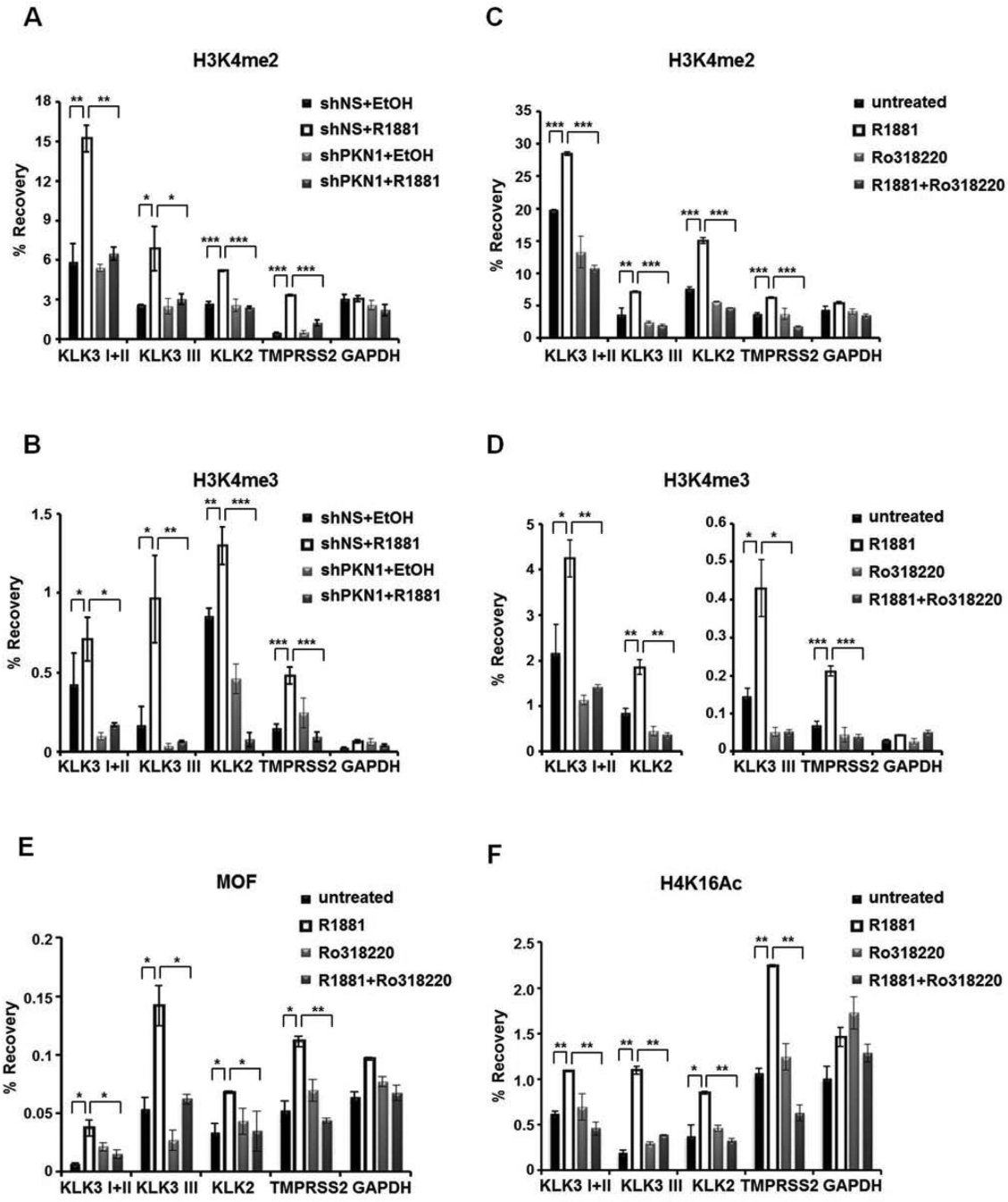


**Figure 4. PKN1 promotes H3K4 methylation and H4K16 acetylation on AR target genes**

(A and B) ChIP was performed using the H3K4me2 (A) or H3K4me3 (B) antibodies using control (shNS) or PKN1 knock-down LNCaP cells grown with or without R1881. (C-F) LNCaP cells were grown in the presence or absence of the PKN1 inhibitor Ro318220 prior to and during R1881 stimulation. ChIP assays were performed with the indicated antibodies at AR target genes. Values represent the mean ± standard deviation of duplicated qPCRs from a representative experiment. Experiments were performed three times with similar results. *p < 0.05; **p < 0.01; ***p< 0.001. See also Figure S5 and Tables S1 and S2.

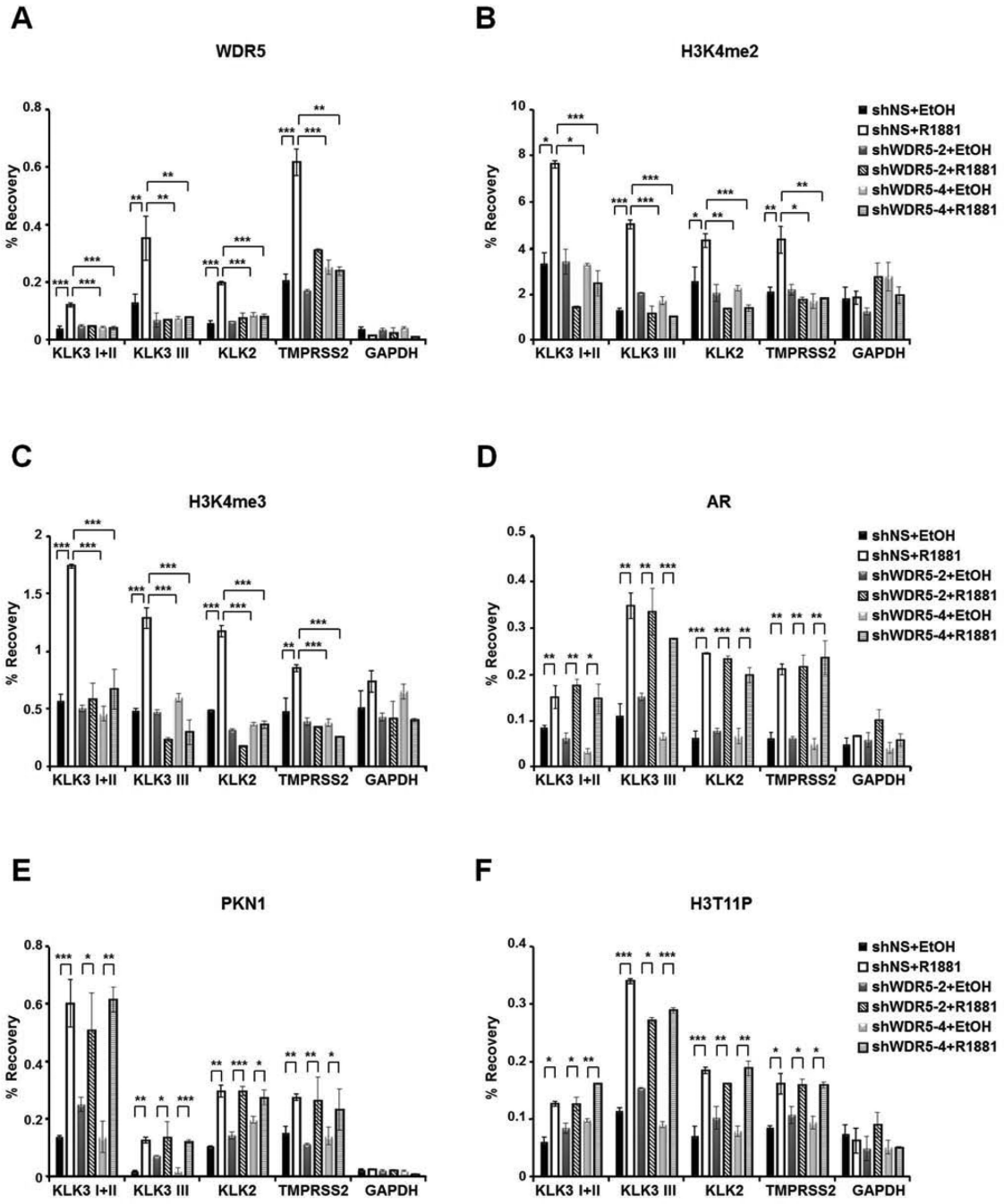


**Figure 5. WDR5 is not required for PKN1 recruitment and H3T11 phosphorylation**

(A-F) Control (shNS) or WDR5 knock-down LNCaP cells were cultivated in the presence or absence of R1881, and analyzed by ChIP using anti-WDR5 (A), H3K4me2 (B), H3K4me3 (C), AR (D), PKN1 (E), or H3T11P (F) antibodies at AR target genes. Values represent the mean ± standard deviation of duplicated qPCRs from a representative experiment. Experiments were performed three times with similar results. *$p < 0.05$; **$p < 0.01$; ***$p < 0.001$.

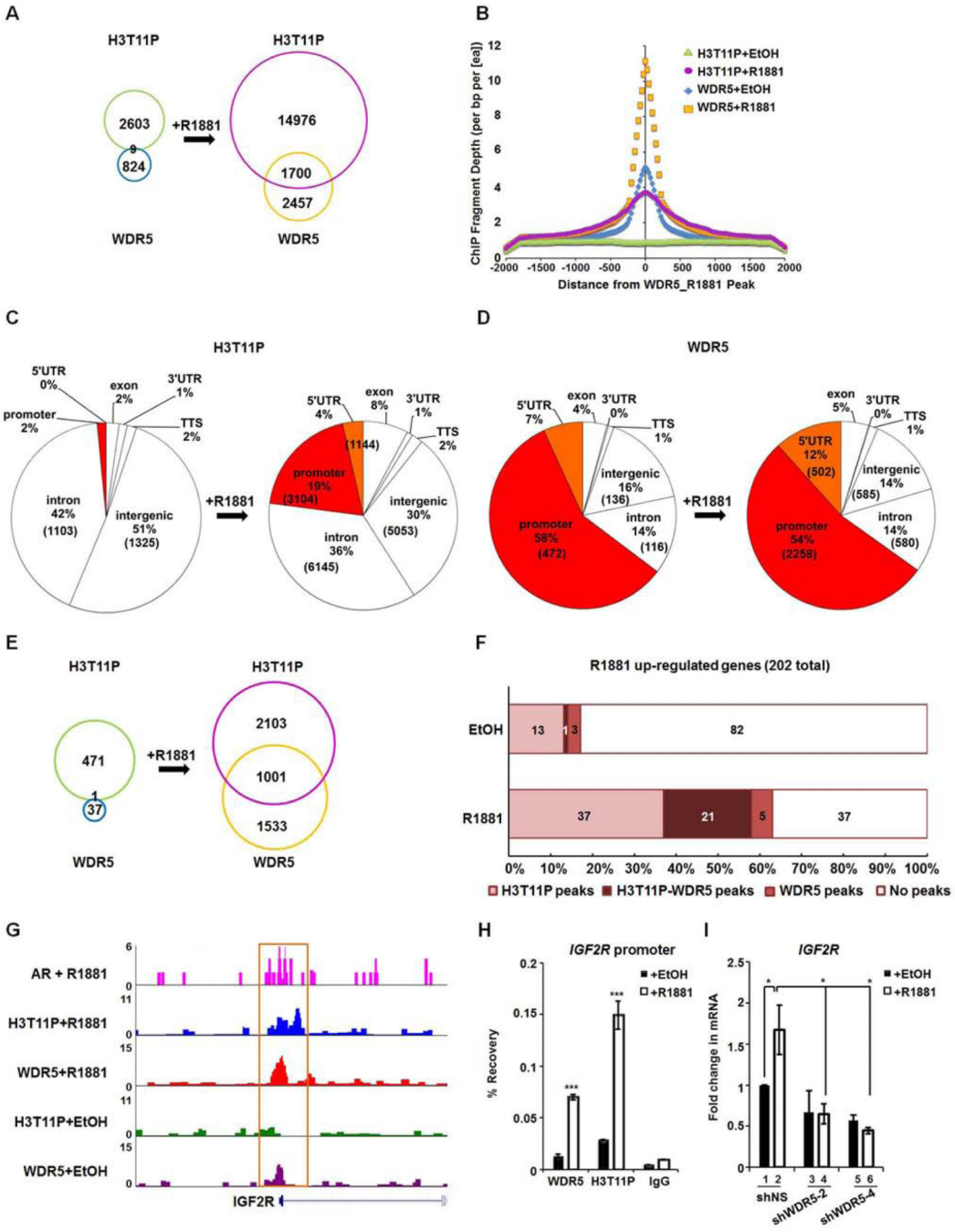


**Figure 6. The genome-wide distribution profiles of WDR5 and H3T11P in hormone treated LNCaP cells**

(A) Area-proportional Venn diagram showing the overlap between WDR5 peaks and areas of H3T11P enrichment in untreated or R1881 treated LNCaP cells based on ChIP-sequencing. (B) Plots of WDR5 and H3T11P ChIP-seq signal intensity relative to the center of WDR5/H3T11P co-occupied sites in untreated or R1881 treated LNCaP cells. (C and D) Pie charts illustrating genomic locations of H3T11P (C) and WDR5 (D) binding sites in the untreated or hormone treated LNCaP cells. (E) Overlap between WDR5 and H3T11P occupancy sites at promoter/5'UTRs identified before and after hormone treatment. (F) Bar

graph represents the overlap between ChIP-seq data for WDR5 and H3T11P peaks compared to genes significantly induced by R1881 treatment (based on RNAseq data from (Tewari et al., 2012)). (G) ChIP-sequencing tracks in unstimulated or androgen stimulated LNCaP cells along the *IGF2R* locus reveals overlapping AR (data from (Yu et al., 2010)) and WDR5 occupancy as well as H3T11P enrichment in the presence of androgen. (H) Recruitment of WDR5 and H3T11P mark at *IGF2R* promoter in R1881 treated LNCaP cells analyzed by ChIP-qPCR. (I) Expression analysis by qRT-PCR of *IGF2R* gene in control and WDR5 knock-down LNCaP cells grown in the presence or absence of R1881. See also Figure S6 and Table S2.

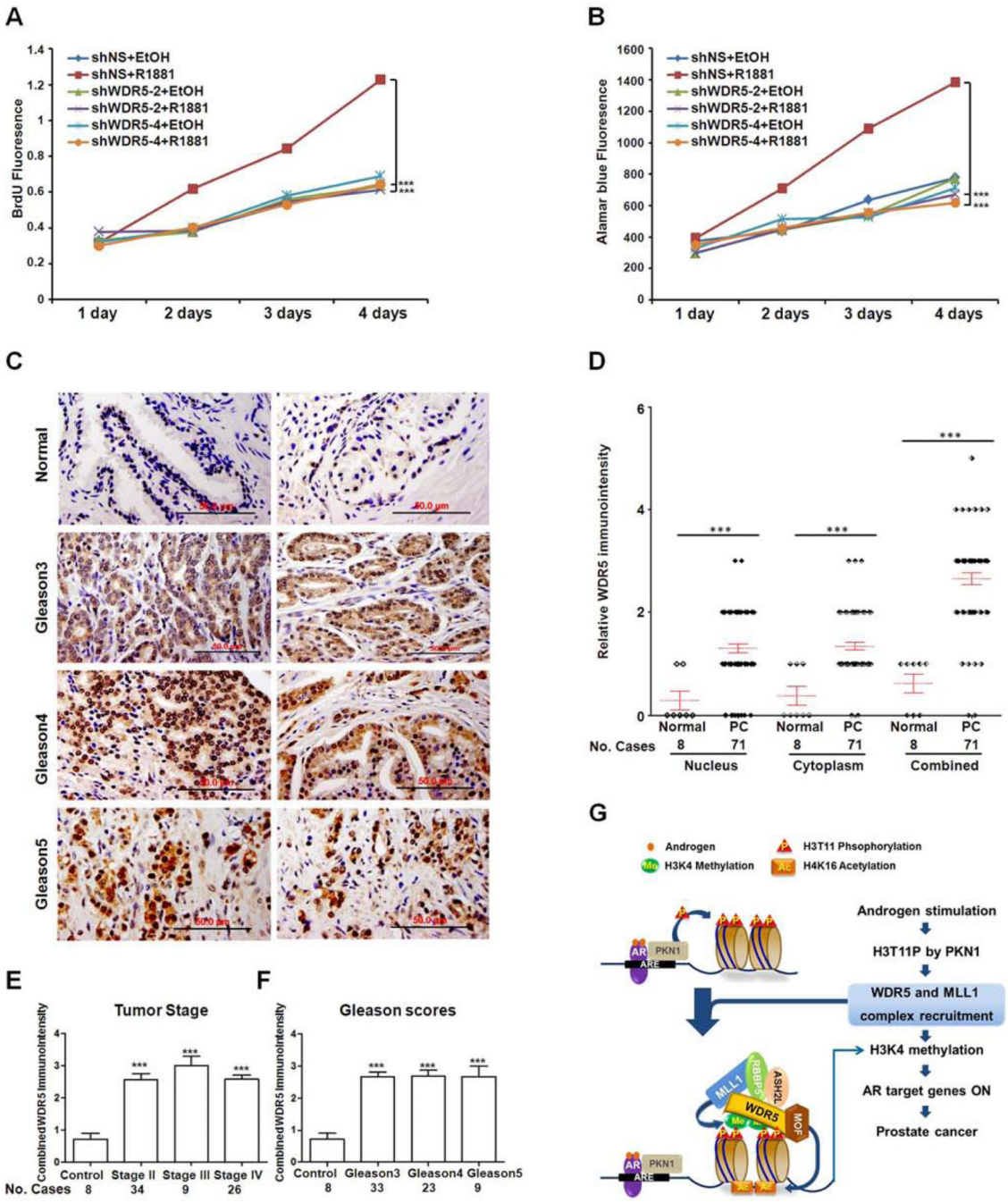


**Figure 7. WDR5 is essential for androgen stimulated cell proliferation and is hyperexpressed in prostate cancer**

(A and B) Control (shNS) or WDR5 knock-down LNCaP cells were grown in presence or absence of AR agonist (R1881). After indicated number of days, BrdU (A) or alamarBlue (B) assays were conducted. Values are represented as mean ± standard deviation. Experiments were performed three times with similar results. ***p< 0.001. (C) Normal (upper panels n=8) or prostate cancer samples (middle and bottom panels, n=71) were analyzed by immunohistochemical staining using anti-WDR5 antibody at 1:350 dilution. 40X magnifications are shown. (D) Semi-quantitative analysis of WDR5 staining in

individual TMA samples. ***p< 0.001. (E) Semi-quantitative analysis of staining of WDR5 expression in normal and tumor stage of II (n=34), III (n=9), and IV (n=26) in TMA samples. ***p< 0.001. (F) Semi-quantitative analysis of WDR5-stained TMA samples by normal and Gleason scores of 3 (n=33), 4 (n= 23), and 5 (n=9). ***p< 0.001. (G) A proposed model highlighting H3T11P-WDR5 interaction in AR target gene regulation, histone modifications, prostate cancer cell proliferation and prostate cancer. See text for details. See also Figure S7.